

# Study of a V-shape flame based on IR spectroscopy and IR imaging

**J. Pouplin, A. Collin, Z. Acem, G. Parent, P. Boulet**<sup>1</sup>

LEMTA, CNRS, Université de Lorraine

2 av. de la Forêt de Haye, TSA 60604 – 54518 Vandœuvre-lès-Nancy Cedex, France

E-mail: pascal.boulet@univ-lorraine.fr

**P. Vena, C. Galizzi, M. Kühni, F. André, D. Escudié**

CETHIL, Campus LyonTech La Doua, INSA de Lyon – CNRS – UCBL - Bât. Sadi Carnot

9, rue de la Physique – 69621 Villeurbanne Cedex

**Abstract.** Applicability of an IR imaging/spectroscopy diagnostic was tested on a laboratory-scale flame. For this purpose, measurements were carried out on a V-shape flame developed along a wall, with the aim of evaluating the wall temperature and of identifying the flame properties (temperature and species concentrations). Infrared measurements with a multiband camera and a spectrometer were post-processed and compared, in particular, with thermocouple measurements carried out for the wall temperature. Simple evaluation involving a correction for the emissivity showed a quite good agreement when assessed against experimental data. An attempt to reconstruct a flame emission spectrum was also carried out, expecting a possible inverse identification of the flame properties. The method showed a promising behaviour on synthetic data built with a radiative transfer model for gas and wall radiation. However, the spectrum reconstruction method is not yet accurate enough to allow an identification of the flame properties in full confidence when applied to actual experimental data. First tests showed a correct qualitative behaviour, but model refinements are required at least for the flame radiation, before getting accurate flame properties.

## 1. Introduction

This study was carried out to test the applicability of an IR imaging/spectroscopy diagnostic to laboratory-scale flames. The diagnostic system was developed by LEMTA in Nancy, and experiments were conducted at the CETHIL in Lyon on a premixed air/methane V-flame. The CETHIL has a wide experience of the combustion in a V-shape flame. This is one of the most common experimental configuration for studying premixed combustion in academic conditions. A premixed flow air / methane is produced in a vertical wind tunnel. The flame is anchored behind a rod and expands freely in the output of the device without confinement [1-2]. Wall-flame interactions were the primary focus of the present study which was mainly aimed at evaluating the surface temperature on the wall where the flame was developing. Such measurement with thermocouples is difficult because of the complex combined transfer at the surface. The CETHIL developed very fine micro-thermocouples, with low inertia, but a confirmation was sought on the provided values. Such verification can be obtained

<sup>1</sup> To whom any correspondence should be addressed.



through infrared measurement. The wall temperature is especially uneasy to evaluate because of the combined contributions of radiation from the flame and from the wall itself, convection at the wall surface and conduction inside the wall thickness. Reflection from the background may be also included as the wall temperature is not expected to reach high values since it is cooled by the inlet air-methane mixing. For this purpose, infrared measurements were first analysed in chosen spectral ranges in order to avoid as much as possible any perturbation by the flame. Then, a model was developed and numerical computations were carried out in order to reconstruct all the radiation measured by a FTIR spectrometer along a line of sight, including the background radiation from the wall itself and the complex radiation from the flame. Such attempts to identify thermal radiative properties based on spectrum reconstruction was already presented by different authors [3-5]. The present study follows the same idea. Experiments were conducted on the setup developed by the CETHIL, involving flame shape reconstruction thanks to laser tomography, infrared flux measurements and data obtained from micro-thermocouples inserted in the wall. These measurements provide a good description of the various thicknesses involved in the numerical simulation and also an idea of the temperature range for the wall, avoiding a blind prediction. Actually, the present flame is quite complicated due to its particular shape, but the combustion conditions are well controlled, which makes the present exercise an interesting test for our method of infrared characterization.

## 2. Experimental setup and methodology

Lean, premixed methane/air V-flames were stabilized at the exit of a 115 x 115 mm square exit nozzle burner. Two 200 x 260 mm ceramic plates were superimposed vertically and oriented parallel to the main flow direction (x-axis in Figure 1 ). The equivalence ratio of the reactants was 0.6, and the mean flow velocity along the exit plane of the burner was 5 m/sec. One laminar and two turbulent flow settings (turbulent intensity 4% and 8%) were studied. Additional details of the apparatus are provided in [6]. Flame topology data were obtained from Mie scattering of olive oil droplets using a Photron FASCAM SA4 1024 x 1024 pixel high speed CCD and CNI MGL-N-532 continuous wave (CW) laser. The oil droplets were generated with a PIVTEC atomizer. Images had a projected spatial resolution of 5 pixels/mm and represented a 200 x 200 mm region of interest in the flame. 500 instantaneous images were acquired for each flame condition and used to determine the mean position of the reactants, highlighted in Figure 2 as the black iso-contour. This was subsequently used, to subdivide the flow “domain ” into reactants, products, and free stream air and correct the separately acquired spectrometer data for variations in mixture composition along the instrument’s line-of-sight. Radiative fluxes were measured with a BRUKER FTIR spectrometer and an ORION infrared camera FLIR SC7000 used with a filter at 3.9 $\mu$ m (a specific wavelength such that no emission occurs by combustion gases, allowing to observe the wall behind the flame throughout the flame). Details on this setup may be found in [7-8]. A typical IR image is shown in Figure 3. Data are given in terms of blackbody equivalent temperature. The wall temperature is increasing with vertical position, as the flame get closer to the wall. Five small white circles are superimposed on the image corresponding to five thermocouple locations, referred to T1 to T5 (from the lowest one at axial position  $x = 60$  mm above the leading edge of the plate to the highest one at axial position  $x = 220$  mm). Only four of these vertical positions were considered for the line of sight used by the spectrometer, as the measurement could not be done on the lowest position. The spectrometer was located in front of the wall, observing a typical area shown by the large white circle in Figure 3 (centred around T5 position in the IR image of Figure 3). The typical shape of the registered spectra is shown in Figure 4 (after post-processing considering a reference spectrum obtained with a high temperature blackbody). Actually three spectra are provided in this case of acquisition in front of the T2 position with a flame obtained for a 4% turbulent premixing of air and methane. They are plotted as rough acquisition data in terms of equivalent blackbody intensities (only converted in intensity with no correction for the wall emissivity and reflectivity effect). As can be seen, the repeatability is quite good and spectra seem to be perfectly superimposed. Peaks due to CO<sub>2</sub> and H<sub>2</sub>O are obvious, as expected in such spectra where the

combustion products are emitting radiation. There is no strong continuous background in the spectrum, except in the low wavenumber range. This is due to the fact that no soot are produced in the flame. Actually, the signal in the low wavenumber range is mainly due to the wall emission, showing that the evaluation of the wall temperature seems to be possible. A comparison with a blackbody spectrum at 420 K is shown in the Figure in order to give an idea of the emission level (which is confirmed by the micro-thermocouples).

Wall emissivity is a crucial data for an evaluation of the real temperature. It was measured on a separate setup with a dedicated spectrometer (Vertex 80 by BRUKER) and an integrated sphere. The spectrum was analyzed, showing a relatively weak spectral evolution as the wall is actually made of ceramic with a black paint on the surface. Planck's average values between 0.94 and 0.95 were found for blackbody sources with temperature in the range 400-500 K (the relevant range for the wall temperature). A particular value of 0.89 was obtained for the wavelength  $3.9\ \mu\text{m}$  (filter of the camera) and the same average value was found for wavenumbers between  $2500$  and  $2700\ \text{cm}^{-1}$  (which is in the same range  $[3.7 - 4.0\ \mu\text{m}]$  and which was of particular interest for some data processing as explained below).

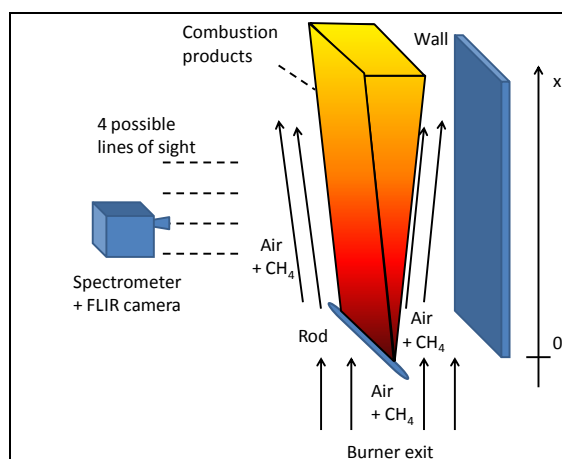


**Figure 1:** sketch of the setup

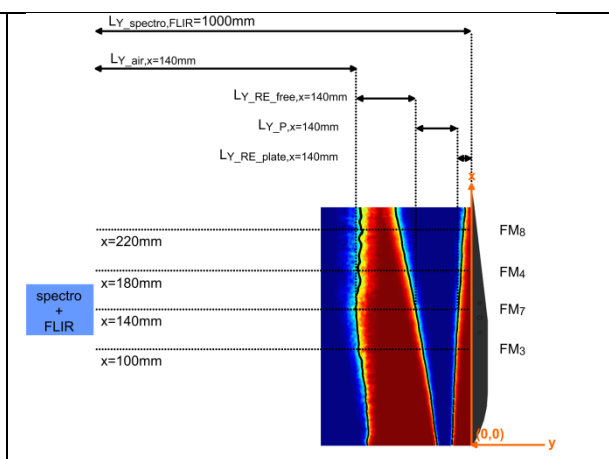


**Figure2:** visualization of the V shape flame from laser tomography analysis. Oil droplet concentration in false colors (maximum concentration in red, zero concentration in blue)

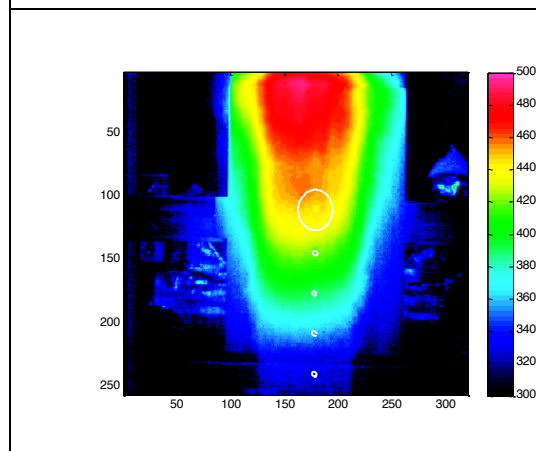


**Figure 3:** Typical IR image of the wall observed throughout the flame. Observation at  $3.9\ \mu\text{m}$ . Data converted in equivalent blackbody temperature (in K on the color bar).

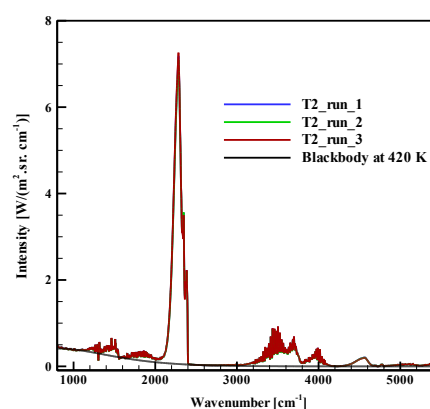


**Figure 4:** Typical IR spectrum. Intensities are plotted for three measurement tests. Case of turbulence 4%.

### 3. Simple identification of the wall temperature

Camera images were post-processed in a quite standard manner involving a correction of the temperature with the emissivity 0.89 in order to account for the deviation from perfect emission by a blackbody and also to bring a correction of the signal due to possible reflection of radiation by the wall from the surroundings. Infrared spectra were also used for a similar first evaluation of the wall temperature, using the experimental data obtained with a resolution of  $4\text{ cm}^{-1}$ . The part of the spectrum between  $2500$  and  $2700\text{ cm}^{-1}$  was chosen for a fit of the intensity considering the following simple model:

$$I = \epsilon_v I_{0v}(T_{\text{wall}}) + (1 - \epsilon_v) I_{0v}(T_{\text{background}}) \quad (1)$$

where  $I_{0v}(T)$  stands for the spectral blackbody intensity at temperature  $T$ . The subscript *background* refers to the surrounding temperature which was set as the ambient one (close to  $20^\circ\text{C}$ ). This spectral range was chosen to avoid any perturbation by the flame (no soot in the flame and no gas influence in this spectral interval). Then, a least mean square method was used to identify the best wall temperature yielding the right intensity profile in this spectral range.

Table 1 gives a comparison between wall temperatures evaluated from spectroscopic measurements, camera image processing and thermocouples. The temperature range  $400$  to  $550\text{ K}$  is confirmed by all the measurement methods. The influence of the premixing conditions is out of the scope of the present paper, but it is also interesting to see that the complex evolution of the temperature is well captured by all the methods (decrease of the temperature level for low turbulence intensity as compared to the laminar case and re-increase for higher turbulence level). Although some discrepancies may appear between the methods for the laminar case, the agreement is quite correct in the two turbulent cases, especially for such a first blind test, that could be now refined.

**Table 1.** Wall surface temperature (in K) at different positions according to camera images, to spectrum fit between  $2500$  and  $2750\text{ cm}^{-1}$  and to micro-thermocouples, for 4 positions on the wall (distance from the leading edge of the plate indicated in mm) and 3 flow conditions of the premixing of air and methane.

	laminar			turbulent 4%			turbulent 8%		
	Camera	Spectro	TC	Camera	Spectro	TC	Camera	Spectro	TC
T2(100mm)	480	478	444	425	425	418	479	464	463
T3(140mm)	514	503	475	450	449	447	518	499	500
T4(180mm)	528	513	489	466	464	459	536	517	517
T5(220mm)	553	538	510	476	476	476	557	538	544

### 4. Radiative transfer model and spectrum reconstruction

For a more sophisticated analysis, the line of sight observed by the spectrometer and the camera was considered and a tentative reconstruction of the spectrum was done. The corresponding radiative transfer model has to take into account radiation from the flame and from the wall. This latter contribution involves emission, but also reflection of the radiation emitted by the flame which is reflected and then partly attenuated during its second path through the flame. A multi-layer model was built following the flame shape observed with tomography and involving: 1) an atmospheric layer between the measurement setup and the flame, 2) a first cold layer of an air-methane mixture injected from the blower, 3) the high temperature region of the combustion products, 4) a second cold layer of air-methane, and the wall itself. Considering the reflection by the wall, each layer emits radiation which is partly redirected through all the successive layers. Hence eight layers are finally considered in a model involving the four layers (1 to 4) cited above and four virtual layers (5 to 8) featuring the

emission toward the plate, reflected, and thus weighted by the wall reflectivity. Following a formulation similar to [6], this yields:

$$I = \sum_{j=5}^8 [\tau(s_j, s) - \tau(s_{j-1}, s)] I_0(s_{j-1}) + \rho \left\{ \sum_{j=1}^4 [\tau(s_j, s) - \tau(s_{j-1}, s)] I_0(s_{j-1}) \right\} + \varepsilon I_0(T_{wall}) \tau(s_{wall}, s) \quad (2)$$

where  $\tau(s_j, s)$  stands for the transmission function of the gas layer between position  $s_j$  and the position of the spectrometer  $s$ ,  $\rho$  and  $\varepsilon$  are the wall reflectivity and emissivity. The subscript  $\nu$  is omitted but the intensity is of course computed for each spectral band.

Gas radiative properties are estimated using a statistical narrow band ( $25 \text{ cm}^{-1}$ ) model based on Malkmus' distribution of linestrengths. Model parameters, developed at CETHIL, were adjusted on LBL curves-of-growth (transmissivities as a function of the path in the gas) following the method described in Ref. [9]. Reference LBL data were generated with the CDSD-4000 spectroscopic database [10] for  $\text{CO}_2$  and HITEMP2010 [11] for  $\text{H}_2\text{O}$  and  $\text{CO}$ . More details about those calculations can be found in Refs. [12-13]. The treatment of non-uniformities involves the Curtis-Godson approximation [14]. This approach is known to raise possible problems of over-correlation in non-isothermal conditions, but it is easy to handle and chosen in the present so as to allow a first evaluation of the method.

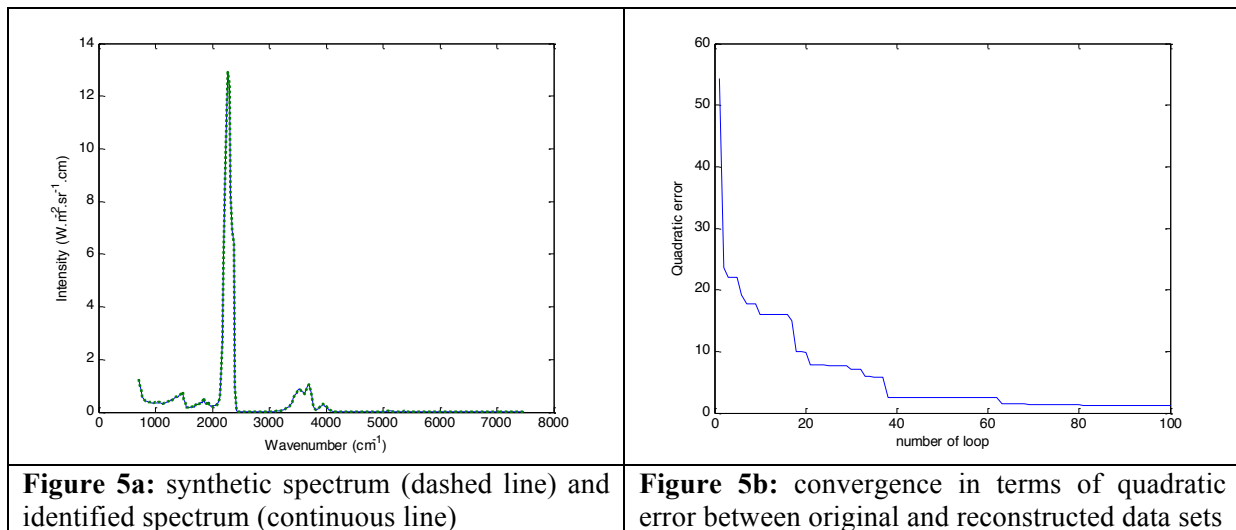
Spectra are built using given inlet properties (gas concentrations, flame temperature, wall temperature) and an optimized set of parameters is sought, such as to provide the best agreement between experimental data and numerical spectrum. A PSO algorithm is used for this purpose (details about the identification method may be found in [15]).

#### 4.1 Validation of the model identification.

A first test was conducted on a synthetic spectrum built with our radiative transfer model used in a direct way. The spectrum was computed based on the following temperatures: 400 K for the wall and 1400 K for the flame, the following concentrations: 20% for  $\text{H}_2\text{O}$ , 10% for  $\text{CO}_2$  and 5% for  $\text{CO}$ , and the respective layer thicknesses: 88.1 cm for the atmospheric layer, 5.9 cm for the first methane plus air layer, 4.4 cm for the combustion product layer and 1.7 cm for the methane plus air layer along the wall (values taken from the experiment when the line of sight is in front of the T2 position, 100 mm above the leading edge of the plate). The wall emissivity was set at the constant 0.95 value. The spectrum was then used as a mock experimental dataset and the identification algorithm was run several times with the following parameters: number of particles 20, number of loops 200.

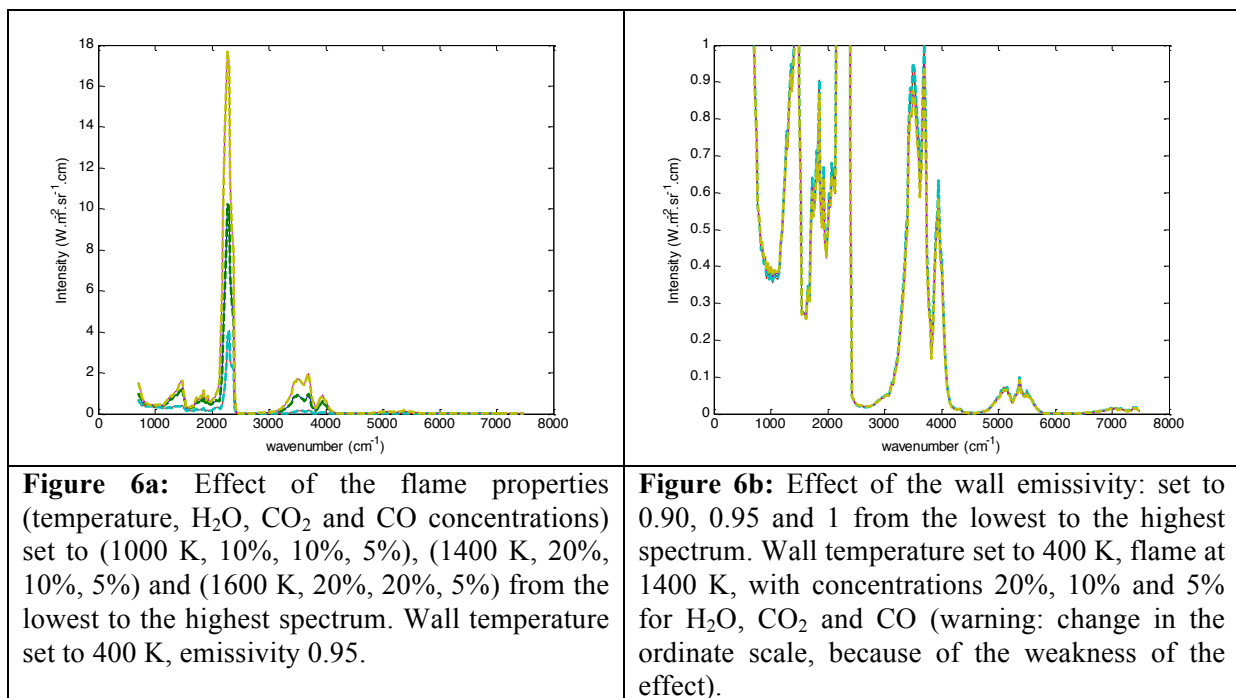
Figure 5a shows the obtained spectra (original data and five identified spectra were all found perfectly super-imposed, showing the perfect behavior of the algorithm in this case of synthetic input data. Figure 5b shows a typical convergence criterion evolution based on the quadratic difference between both datasets as a function of the loop number.

It is known that such a test is not fully convincing because the same model is used in direct and inverse ways. However it shows that the numerical parameters and the identification algorithm are at least performing well. The wall temperature was found with an accuracy better than  $1^\circ\text{C}$  for all runs and all the flame properties (temperature and gas concentrations) were found with a very satisfying accuracy (for example for the first run: 1399 K for the flame with the following concentrations: 10.2% for  $\text{H}_2\text{O}$ , 20.1% for  $\text{CO}_2$ ). Of course the estimations could be even further improved increasing the identification parameters (numbers of particles and loops).



#### 4.2 Sensitivity study.

A sensitivity study was carried out still with the same method (generation of synthetic data and blind search for optimal conditions yielding the best fit in terms of spectra). Eight different cases were tested which were defined as to bracket the reference case seen above, always keeping the same geometry. The flame properties (Figure 6a), then the wall properties (Figure 6b for the wall emissivity and Figure 6c for the wall temperature), were varied in order to investigate if some conditions could penalize the ability to identify the wall temperature and the flame characteristics. The emissivity influence is plotted with a particular scale on the Y-axis (Figure 6b) since the influence of this parameter is very weak (as it even hardly appears despite the chosen scale). This also shows that this parameter has no major effect on the spectra. In all subfigures synthetic data are plotted with thin continuous lines and identified spectra are plotted with thick dotted lines, such that it appears that the spectra are apparently perfectly reconstructed since no discrepancy appear between two curves (synthetic and identified) corresponding to the same case study.



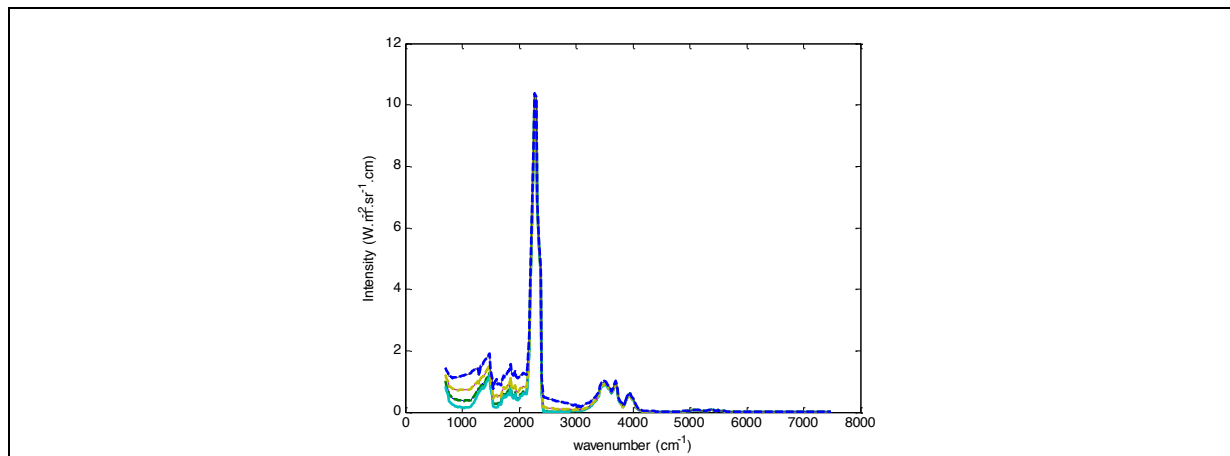


**Figure 6c:** Effect of the wall temperature: 300 K, 400 K, 500 K, 600 K from the lowest to the highest spectrum. Emissivity 0.95, flame at 1400 K, with concentrations 20%, 10% and 5% for  $\text{H}_2\text{O}$ ,  $\text{CO}_2$  and  $\text{CO}$ .

**Figure 6:** sensitivity study on the identification algorithm, comparison between synthetic data (thin continuous lines) and identified spectra (thick dotted lines, in all cases superimposed on the corresponding continuous lines)

What was especially satisfactory in this numerical exercise is that the maximum discrepancy on the temperature identification never exceeded 1 K as compared to the original value, whatever the case, either on the wall or the flame temperature. Similarly, synthetic and identified concentrations were found in a very good agreement (always below 1% of absolute discrepancy).

#### 4.3 Results for experimental data treatment and discussion.

The method based on spectrum reconstruction and property identification was then applied on the measured spectra. The experimental data were first averaged on  $25 \text{ cm}^{-1}$  bandwidths, in accordance with the model discretization. The case of the turbulent mixing at 4% was used, the same conditions being kept as in the validation case in terms of geometry and of numerical parameters used in the PSO algorithm. The comparison between experimental data and a typical identified spectrum is presented in Figure 7a.

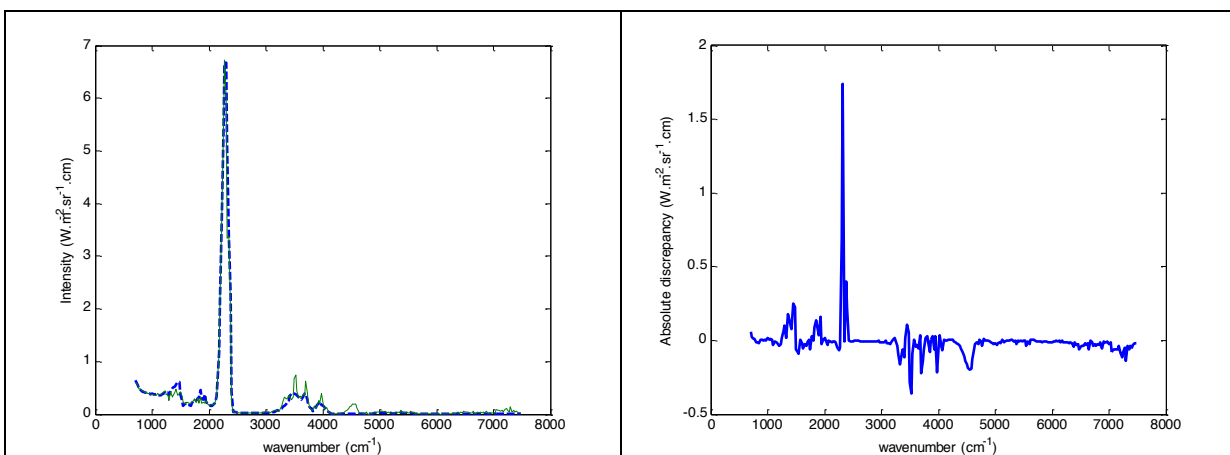


**Figure 7a:** Experimental dataset and reconstructed spectrum based on the search for optimal flame properties.

**Figure 7b:** Absolute discrepancy between experimental and reconstructed spectrum

It seems that the spectrum is qualitatively reconstructed, but with some discrepancies in the peaks attributed to the gases. The discrepancies are plotted in Figure 7b, revealing quite large errors which were not so obvious on the spectrum itself. Such discrepancy does not allow an identification of the flame in confidence. The identification exercise was repeated several times, also varying the number of loops in the PSO algorithm (up to 400 loops, with apparent convergence reached considering the quadratic error between experimental and numerical spectra). It was found that the identified temperature and gas concentrations were slightly varying, but an average prediction could be done on the flame properties. Spectra are not plotted because they provide exactly the same figure as Figure 7a. The average discrepancy between two identified spectra was typically below  $0.01 \text{ W.m}^{-2}.\text{sr}^{-1}.\text{cm}$  (when averaged over the whole spectral range), with a maximum local value between the two extreme identifications around  $0.2 \text{ W.m}^{-2}.\text{sr}^{-1}.\text{cm}$  (found in the  $\text{CO}_2$  peak).

Regarding the identified properties, average data based on five runs were found as follows (with maximum discrepancy as compared to the average value indicated between parenthesis): temperature 1617 K (+/- 41 K),  $\text{H}_2\text{O}$  concentration 5.3% (+/-0.4%),  $\text{CO}_2$  concentration 3.3% (+/-0.2%). CO concentration was apparently very low (around 0.2%). The wall temperature was found with less uncertainty: average value 409 K (+/- 5K). This is in a correct agreement with the other estimations, as presented above. For the flame temperature however, 1617 K is probably an overestimated value, owing to the experience of present authors involved in such flame study. The problem is that with the present model a compensating effect may affect the results since a too high temperature may be compensated by too low concentrations. At this stage we consider that the method could work well but improvements are required, in particular in terms of gas radiation modeling. A specific model, combining results from the Generalized  $k$ -moment method [16] together with the Multi-Spectral Framework [12] is presently developed at CETHIL for this task. Those methods were studied separately and found to provide very high accuracies when compared to LBL reference calculations both in uniform and non-uniform media. Implementing this more accurate model is likely to improve the accuracy of the outputs (in terms of temperature and species concentrations) of the inversion scheme.

As the wall temperature was the main parameter sought here and since it was obtained with less uncertainty, a systematic identification was performed on all cases, yielding the values reported in table 2. As can be seen, the agreement with the thermocouple measurements is not as good as the one observed with the data extracted from the experimental spectra and IR images, but results are still in the same range. Identified temperatures are lower as compared to the straightforward estimation (table 1). It seems that the discrepancies in the gas peaks due to the limitations of the model result in compensating deviations for the continuous background attributed to the wall. This is because the optimization is converging toward a compromise which minimizes the discrepancies over the whole wavenumber range, with overestimations and underestimations depending on the wavenumber.

**Table 2.** Wall temperature (in kelvins) at different positions based on complete spectrum reconstruction compared with data from micro-thermocouples, for 4 positions (x-position in mm) on the wall and 3 flow conditions of the premixing of air and methane.

	laminar		turbulent 4%		turbulent 8%	
	Identification	TC	Identification	TC	Identification	TC
T2(100 mm)	469	444	409	418	446	463
T3(140 mm)	492	475	435	447	478	500
T4(180 mm)	503	489	448	459	495	517
T5(220 mm)	523	510	459	476	512	544



Hence, the method seems to be a good idea but some refinements of the radiation model will be necessary. In particular, the model will have to address in a better way the heterogeneities in terms of concentrations and temperature.

## 5 Conclusion

An identification method of wall temperature and flame properties was tested on a V-shape flame, based on the post-processing of radiative transfer measurements. The idea was to reconstruct the best spectrum fitting the experimental data obtained on a real experiment and to identify the required experimental parameters. The method was shown to perform well on synthetic data produced with a SNB model for the gas radiation (also involved in the identification method). However, this must be considered with limited confidence, since this calibration is what is called an “inverse crime” because the same model is used for the data generation and the inverse identification. This is of course easier than working on real data with their noise, uncertainties and particular spectral resolution. When applied on real data, the reconstructed spectra showed a satisfying global shape but with significant discrepancies in the gas peak ranges. This was suspected to penalize the identification of the flame properties. The wall temperature was found with a better confidence and various evaluations were found in a satisfying agreement, owing to the measurement difficulties with the different methods: thermocouples, IR imaging or spectrometry. The goal of this collaborative work is still to go toward a complete flame characterization. This will require an improved gas radiation model in particular.

## References

- [1] C. Galizzi and D. Escudié. Experimental analysis of an oblique turbulent flame front propagating in a stratified flow, *Combustion and Flame*, 157, pp. 2277-2285, 2010.
- [2] H. Guo, B. Tayebi, C. Galizzi and D. Escudié. Burning rates and surface characteristics of hydrogen-enriched turbulent lean premixed methane-air flames, *International Journal of Hydrogen Energy*, 35, pp. 11342-11348, 2010.
- [3] Y. Billaud, P. Boulet, Y. Pizzo, G. Parent, Z. Acem, A. Kaiss, A. Collin and B. Porterie. Determination of woody fuel flame properties by means of emission spectroscopy using a genetic algorithm. *Combustion Science and Technology*, 185, pp. 579-599, 2012.
- [4] A. Soufiani, J.-P. Martin, J.-C. Rolon and L. Brenez. Sensitivity of temperature and concentration measurements in hot gases from FTIR emission spectroscopy. *Journal of Quantitative Spectroscopy and Radiative Transfer*, 73, pp. 317-327, 2002.
- [5] F. André, R. Vaillon, I. Ayranci, D. Escudie and N. Selcuk. Radiative transfer diagnostic technique of sooting flames from emission spectroscopy. In: *Proceedings of the Fourth International Symposium on Radiative Transfer*, Istanbul, Turkey, June 20-25, 2004.
- [6] P. Vena, C. Galizzi, F. André, M. Kuhni and D. Escudié. Experimental study of flame-wall interaction: focus on the propagation of a premixed front near a wall, *23rd International Symposium on Transport Phenomena*, Auckland, New Zealand, 19-22 November 2012.
- [7] G. Parent, Z. Acem, S. Lechêne and P. Boulet. Measurement of infrared radiation emitted by the flame of a vegetation fire. *International Journal of Thermal Sciences*, 49, pp. 555-562, 2010.
- [8] P. Boulet, G. Parent, Z. Acem, B. Porterie, A. Kaiss, Y. Billaud, Y. Pizzo and C. Picard. Experimental investigation of radiation emitted by optically-thin to optically-thick wildland flames *Journal of Combustion*, vol. 2011, Article ID 137437.
- [9] J. Taine and A. Soufiani. Gas IR radiative properties: from spectroscopic data to approximate model. *Advances in Heat Transfer*, 33, pp. 295-414, 1999.
- [10] S.A. Tashkun and V.I. Perevalov. CDSD-4000: High-resolution, high-temperature carbon dioxide spectroscopic databank. *Journal of Quantitative Spectroscopy and Radiative Transfer*, 112, pp. 1403-1410, 2011.
- [11] L.S. Rothman et al. HITEMP, the high-temperature molecular spectroscopic database. *Journal of Quantitative Spectroscopy and Radiative Transfer*, 111, pp. 2139-2150, 2010.

- [12] F. André, L. Hou, M. Roger and R. Vaillon. The multispectral gas radiation modeling: a new theoretical framework based on a multidimensional approach to  $k$ -distribution methods, Journal of Quantitative Spectroscopy and Radiative Transfer, 147, pp. 178-195, 2014.
- [13] F. André, L. Hou and V.P. Solovjov. An exact formulation of  $k$ -distribution methods in non-uniform gaseous media and its approximate treatment within the Multi-Spectral framework, accepted in the proceedings of the present Eurotherm seminar, 2015.
- [14] S.J. Young. Nonisothermal band model theory. JQSRT Vol. 18, 1977, pp. 1-28.
- [15] M. Clerc. Particle Swarm Optimization. ISTE Publishing Company, London, UK, 2006.
- [16] F. André, V.P. Solovjov, L. Hou, R. Vaillon and D. Lemonnier. The generalized  $k$ -moment method for the modeling of cumulative  $k$ -distributions of H<sub>2</sub>O at high temperature. Journal of Quantitative Spectroscopy and Radiative Transfer, 143, pp. 92-99, 2014.